3A.1 Introduction

ZnO nanostructures like nanorods, nanowires, nanonails, nanodisks, nanoribbons and so on have been fabricated by different solution-phase methods such as sol-gel, template-based, tamplateless etc. The size and shape of nanoparticles can be varied by controlling the parameters during synthesis like pH, temperature and precursor concentration [1]. Under strong alkaline conditions, excess OH^- ions adsorb on the surface and inhibit the growth which results in morphology transition. Li group/ et al. reported flower like ZnO microstructures by alkaline hydrolysis of zinc chloride and sodium hydroxide [2]. Sakohara et al. repoted OH^- or organic groups on the surface of the particles affect the intensity of the emissions in liquid media [3].

The luminesence properties of ZnO material can be enhanced by decreasing the particle size. ZnO nanostructures show enhanced visible light emission due to quantum size confinement [4], increase of surface area [5] and increase of oxygen vacancies [6]. It has been reported that spectral position and the intensity of the visible emission also depend on the fabrication process [7].

In this study, we report the synthesis of ZnO nanostructures of different shapes by simple wet chemical method using DL(±) tartaric acid as capping agent at relatively low temperature. We have studied the variations of the synthetic parameters like concentration of capping agent and precence of surfactants like sodium dodecyl sulfate (SDS) and cetyltrimethylammonium bromide (CTAB) as additives on the size and morphology of the nanoparticles. We have also studied the optical and suface stabilization of the as-synthesized nanostructures.

3A.2 Materials

Analytical Grade zinc nitrate $Zn(NO_3)_2.6H_2O$, Sodium dodecylsulphate (SDS), Cetyltrimethylammonium bromide (CTAB), sodium hydroxide NaOH, were obtained from S D Fine-Chem Mumbai. DL(±)-Tartaric acid ($C_4H_6O_6$) for synthesis was

obtained from Loba Chemie Pvt. Ltd. Mumbai, India. All the chemicals were used as received.

3A.3 Synthesis

Synthesis of nanoflowers

In a round bottom flask 5 ml (0.1M) $Zn(NO_3)_2$, 5 ml (0.01M) of tartaric acid (TA) solution and 35ml distill water was added. The reaction mixture was stirred for half an hour and temperature was maintained at 70°C. To this reaction mixture added 5mL 0.5 M NaOH drop-wise at rate 1ml per minute. The temperature of the reaction mixture was maintained for half an hour and then allowed to cool naturally.The resulting reaction mixture was kept under stirring for 24 hours. The resulting dispersion was centrifuged at 1000 rpm and washed with distill water several times. The product was dried at 100°C.

Synthesis of Naoflower with small petals

In this synthesis the concentration of tartaric acid was increased to 0.05 M and other parameters were same as in above method.

Synthesis of Chloroplast-like ZnO nanostructures

In this synthesis ZnO nanoparticles were synthesized in absence of tartaric acid while other parameters were same as above method.

Synthesis of prism shaped nanostructures

In a round bottom flask 5 ml (0.1M) $Zn(NO_3)_2$, 5ml (0.01M) CTAB, 5 ml (0.01M) of tartaric acid solution and 30ml distill water was added. The reaction mixture was stirred for half an hour and temperature was maintained at 70°C. To this reaction mixture added 5mL 0.5 M NaOH drop-wise at rate 1ml per minute. The temperature of the reaction mixture was maintained for half an hour and then allowed to cool naturally. The resulting dispersion was centrifuged at 1000 rpm and washed with distill water several times. The product was dried at 100°C.

Synthesis of armed chloroplast shaped nanostructures

Instead of CTAB solution 0.01 M SDS was added and rest of the parameters were same as above method.

3A.5 Result discussion

X-ray diffraction (XRD)

The purity and crystalline properties of ZnO nanostructures were studied powder X-ray diffraction (XRD). The XRD pattern are shown in Figure 3A.1. The diffraction peaks were observed at 2θ 31.7, 34.3, 36.2, 47.4, 56.5, 62.7, 66.3, 67.8, 69.0, 72.4 and 76.8 all diffraction peaks can be ascribed to ZnO in the wurzite structure hexagonal phase (JCPDS card no 89-1397). The sharp and strong peak indicate that product is well crystallized. The width of the peaks are quite broader compared to the bulk, which shows particles in nano regime. The particle size was calculated using Debeye-Scherrer formula [8], the average nanocrystallite size for ZnO was in the range of 17-50 nm as shown in Table. 3A.1.

Energy Dispersive X-ray (EDX)

The elemental composition of as-synthesized nanostructures was studied by Energy Dispersive X-ray (EDX) analysis as shown in Figure 3A.2. The composition of the as-synthesized nanostructure is given in the Table. 3A.2. The Zn/O ratio shows stoichiometry product.

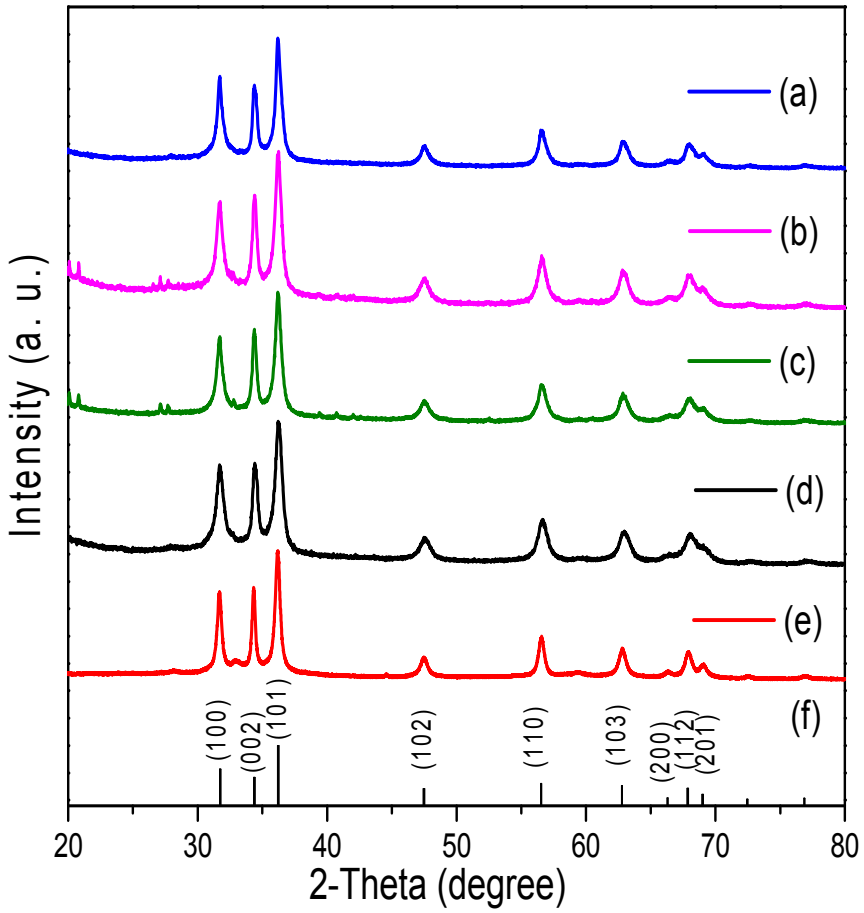

Figure 3A. 1. X-ray diffraction pattern of ZnO nanoparticles synthesized in different concentration of capping agent (a) chloroplast like ZnO (No TA) (b) Nanoflower (0.01M TA) (c) Nanoflowers with small petals (0.05M TA) (d) prism-like (0.01M TA and 0.01M CTAB) (e) armed-chloroplast-like (0.01M TA and 0.01M SDS) (f) bulk ZnO standard (JCPDS card no. 89-1397).

Table no. 3A.1. Absorption edge and particle size from XRD.

Morphology of ZnO nanostructures	UV (nm)	Particle size from XRD (nm)
Nanoflower (0.01M TA)	372	44.1
Nanoflowers with small petals (0.05M TA)	371	46.0
chloroplast-like (No TA)	386	50.2
prism-like (0.01M TA) and 0.01M CTAB)	382	50.2
armed-chloroplast like (0.01M), (0.01M SDS)	366	17.9

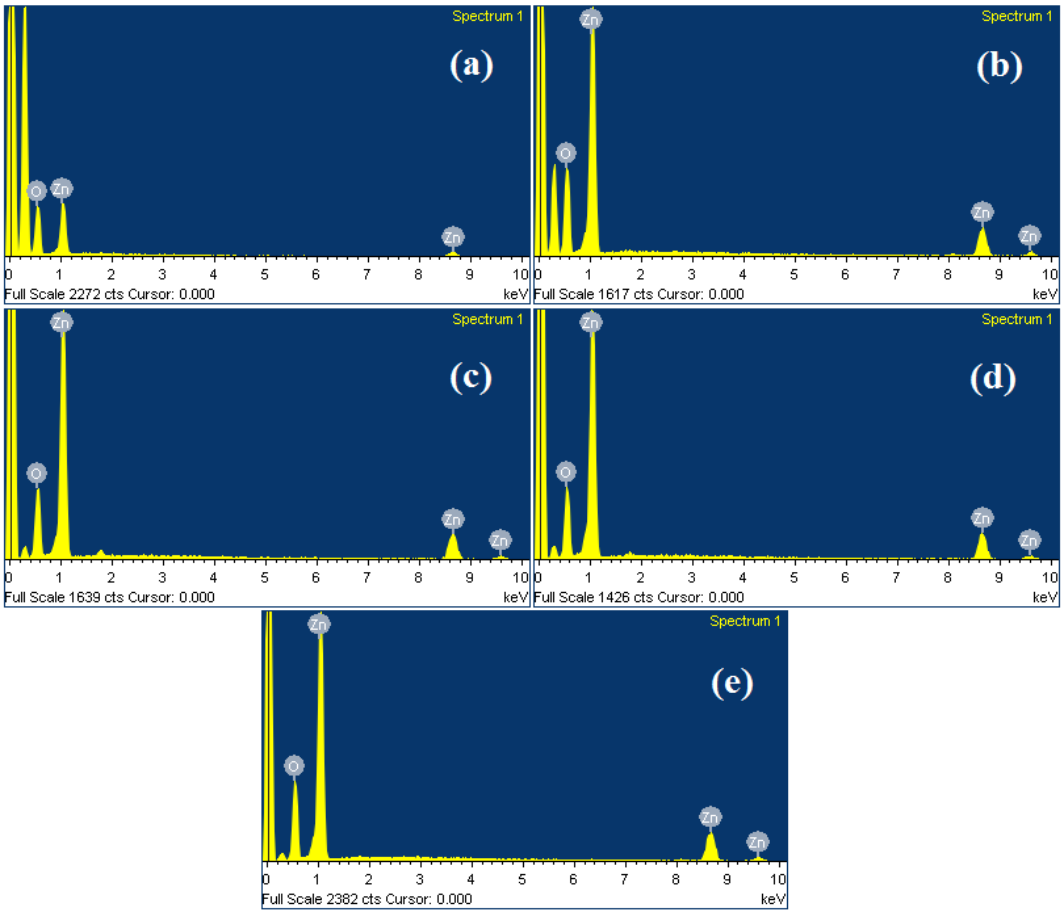

Figure 3A. 2. EDX of ZnO nanoparticles synthesized in different concentration of capping agent (a) Nanoflower (0.01M TA) (b) Nanoflowers with small petals (0.05M TA) (c) prism-like (0.01M TA and 0.01M CTAB) (d) armed-chloroplast-like (0.01M TA and 0.01M SDS) (e) chloroplast like ZnO (No TA).

Table 3A.2. Elementary composition of the ZnO nanoparticles as studied by EDX.

Samples	Zn (At.%)	O (At.%)	Zn/O
(0.01 M TA)	20.66	79.34	0.26
Nanoflowers with small petals (0.05M TA)	35.52	64.48	0.55
chloroplast-like (No TA)	38.74	61.26	0.63
(0.01 M TA) and CTAB	40.83	50.17	0.81
(0.01 M TA) and SDS	40.91	59.09	0.69

Morphology analysis

The size and morphology of the ZnO nanoparticles was studied by transmission electron spectroscopy (TEM) as shown in Figure 3A.3. The TEM analysis shows that morphology of ZnO NPs is strongly dependent on synthetic parameters. In the absence of tartaric acid as the capping agent, chloroplast-like nanostructures were obtained of dimension in the range 250-800 nm (Figure 3A.2a). Few chloroplasts-like nanostructures were formed by fusion of two or three smaller chloroplasts at the center while individual tapering end can be observed. These chloroplast nanostructures seem to be composed of fine nanorods.

In the formation of chloroplast shaped nanostructures, Zn^{2+} and OH^- must have played key role as no capping agent was used during synthesis. Li and co-workers reported a template- and surfactant-free aqueous solution route for flower-like ZnO microstructures [9]. They reported fast nucleation-growth kinetics for the formation of ZnO nanoflowers. Yu et al. reported ZnO nanotube bundle composed of closely packed nanotubes. They proposed coexistence of growth and selective dissolution of metastable Zn-rich (0001) polar surfaces of ZnO as possible growth model [10]. Cho et al. reported 3D ZnO superstructures with building blocks like nanoplates, 1D and cones-like using sodium peroxide [11]. Similar type of growth pattern could be there in the chloroplast-like ZnO nanoparticles in absence of capping agent.

ZnO nanostructures of different morphologies were obtained in presence of tartaric acid as a capping agent. In presence of 0.01M (DL) tartaric acid as capping agent, one can observe nanoflowers of size in range 360-500 nm (Figure 3A.1a-b). These ZnO nanoflowers seem to be constructed of thin rods as the building blocks.

Zhang et al. reported flowerlike, disklike, and dumbbell-like ZnO microcrystals using ammonia, citric acid (CA), and poly(vinyl alcohol) (PVA) as the capping molecules [12]. Pal et al. reported synthesis ZnO flower like structures by controlled content of ethylenediamine and pH of the reaction mixture [13]. They revealed that flower like structures were formed of conical nanorods and some fiber like planar structures of about 1 μm average length.

On increasing the concentration of tartaric acid from 0.01M to 0.05 M flower-like nanostructure with small length of petals were obtained (Figure 3A.2c). The dimensions of these nanoflowers were in the range 750-950 nm. We can observe an increase of the size of the ZnO nanostructures on increase of the concentration of tartaric acid as a capping agent. The increase of size of nanostructures with increase in the amount of tartaric acid could be due to some chemical binding of adsorbed tartaric acid.

The effect of presence of additives such as CTAB and SDS in presences of tartaric acid as capping agent on the morphology of ZnO nanostructures was also studied. In presence of 0.01 M tartaric acid and 0.01 M CTAB prism-like morphology was obtained. The average size of prism-like nanostructures was in the range 450-550 nm (Figure 3A.4). In presence of 0.01 M tartaric acid and 0.01 M SDS, small-armed-chloroplast shaped nanostructures were obtained (Figure 3A.4b). The average size of prism-like nanostructures was in the range of length ~300 nm and breadth ~130 nm. From the TEM analysis we can conclude that morphology of nanoparticles can be tuned by varying the synthetic parameter like concentration of alkali, tartaric acid as capping agent and presence additives like CTAB and SDS as shown in schematic diagram 2.

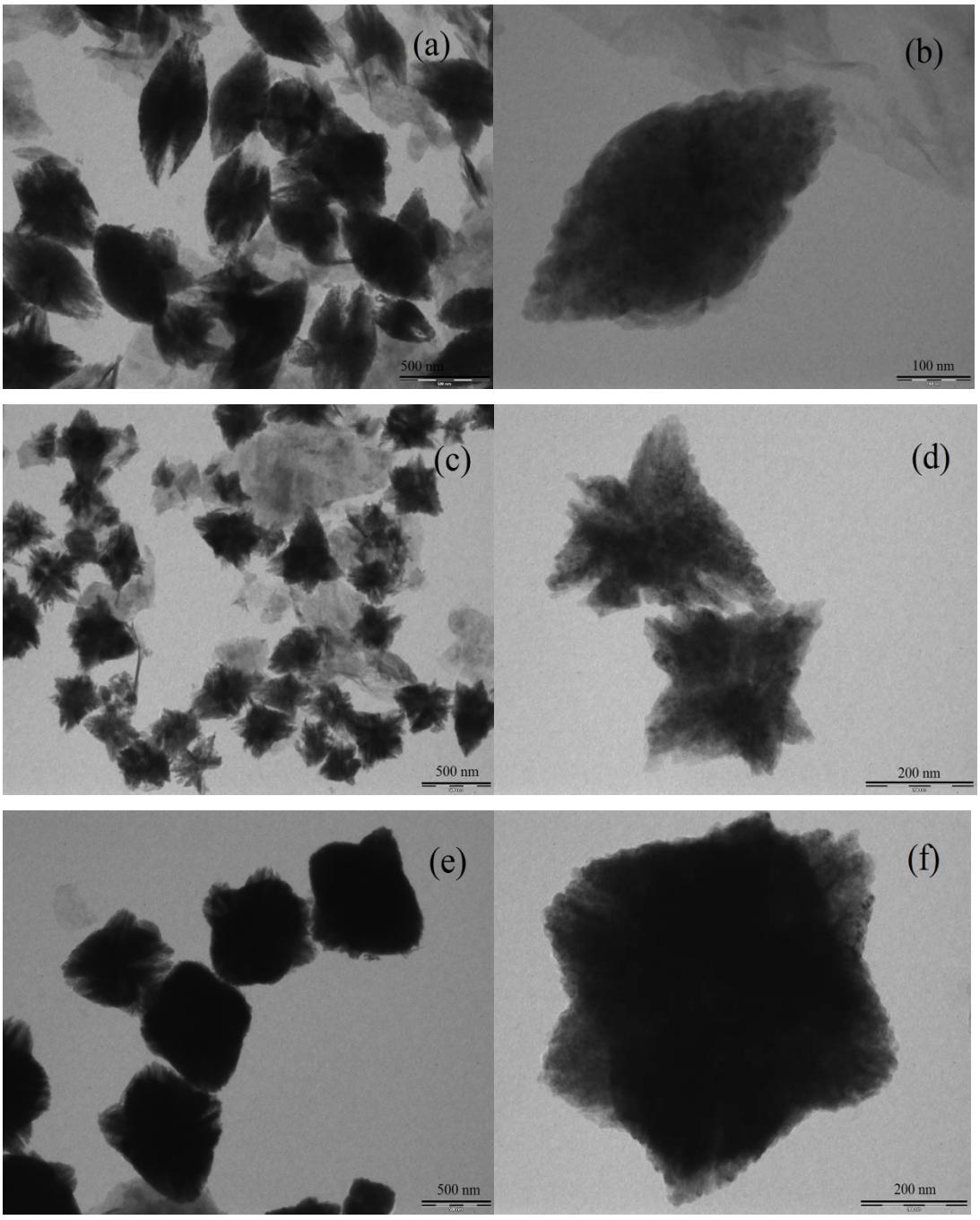

Figure 3A.3. TEM micrographs of ZnO nanoparticles with (a,b) No TA (c,d) 0.01M TA (e,f) 0.05M TA.

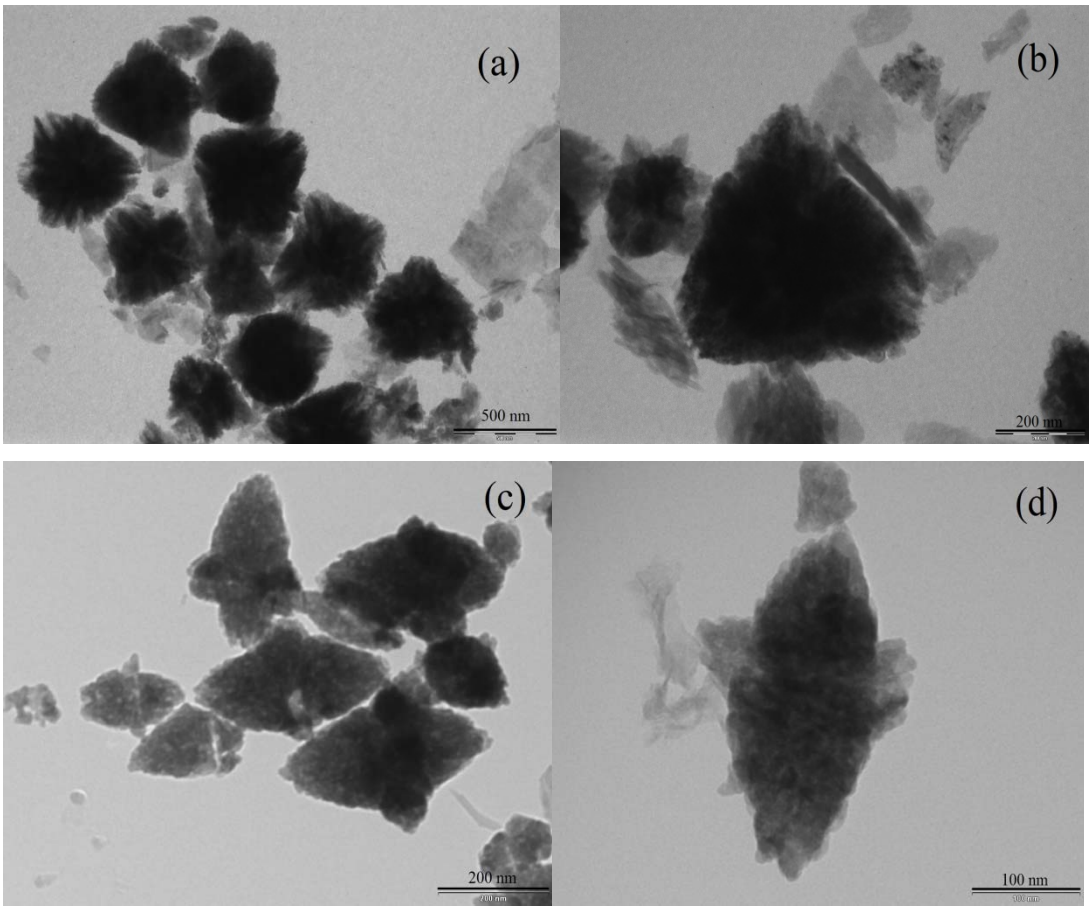

Figure 3A.4. TEM images in precence of tartaric acid and additives (a,b) 0.01M TA and 0.01M CTAB and (c,d) 0.01M TA and 0.01M SDS.

Dynamic light scattering (DLS) and zeta potential

Dynamic light scattering (DLS) was carried out to validate the particle size. It gives particle size in the terms of hydrodynamic diameter and its values for as-synthesized NPs is given in the table no. 1 which is in agreement with the TEM results. The highest hydrodynamic diameter was obtained in ZnO nanoflowers with small petals. The particle size as obtained from DLS analysis is shown in Figure 3A.5.

We have also measured the surface charge stabilization of nanoparticles using zeta potential of the dispersed particles by dynamic light scattering (DLS) as shown in Figure 3A.5(f). Zeta potential values of all the as-synthesized ZnO nanoparticles were

negatively charged of different magnitude and it is given in the Table 3. Berg et al. reported electrostatic stabilization requires zeta potentials of at least ±30 mV [14]. Flower-like ZnO nanostructures showed highest negative charge (-23.97 mV) in comparision to the other morphologies. The negative surface charge indicates OH^- and tartaric acid could be adsorbed to stabilize the surface of the nanostructures.

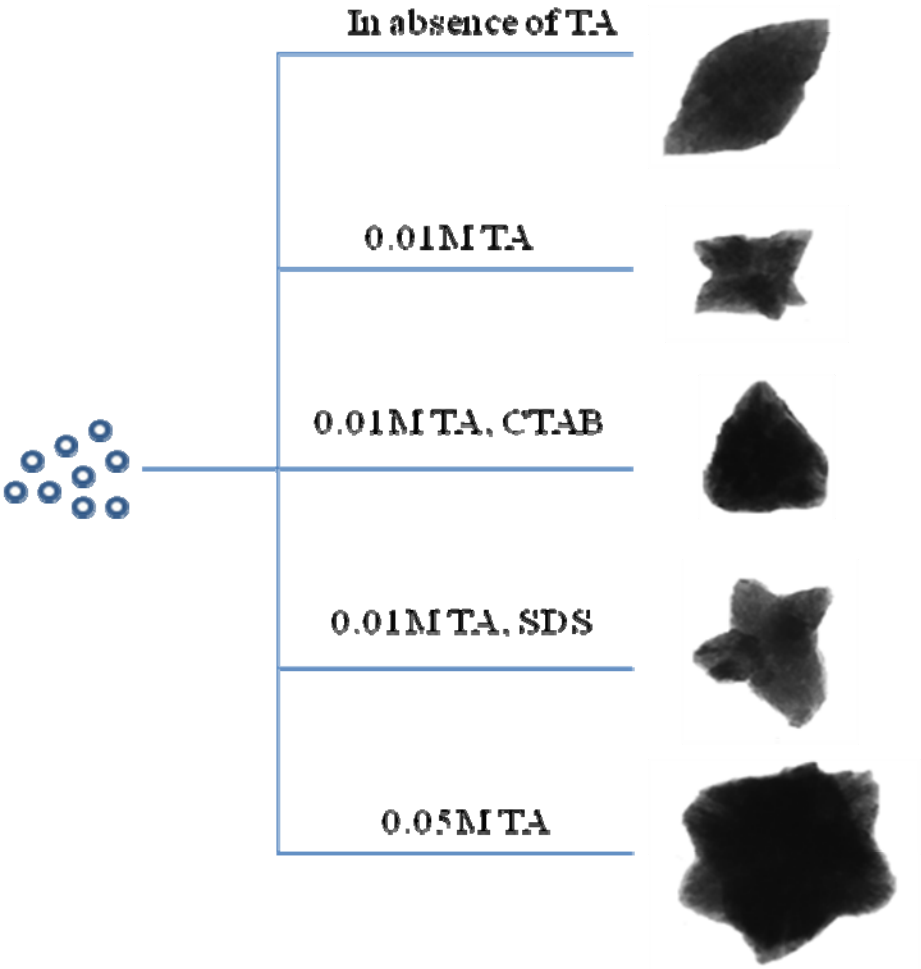

Schematic diagram. 2 Morphology of nanoparticles can be tuned by varying the synthetic parameter like concentration of tartaric acid as capping agent and presence additives like CTAB and SDS.

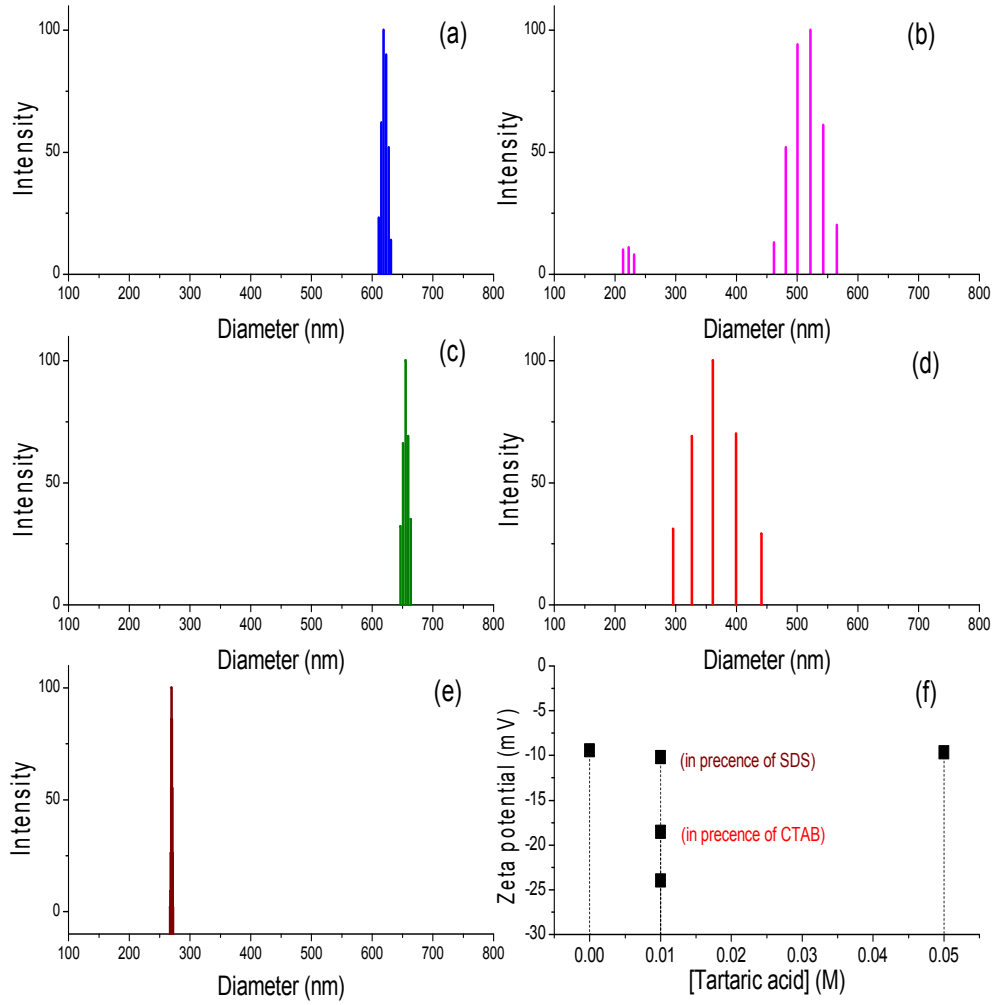

Figure 3A.5. Hydrodynamic diameter by dynamic light scattering of ZnO nanoparticles with (a) No TA (b) 0.01M TA (c) 0.05M TA (d) 0.01M TA and 0.01M CTAB (e) 0.01M TA and 0.01M SDS and (f) Zeta potential of nanostructures synthesized in different concentration of TA and surfactants as additives.

Table. 3A.3 Hydrodynamic diameter and Zeta potential of ZnO nanoparticles studied by Dynamic light scateering (DLS).

ZnO nanoparticles	particle size (Dynamic light scattering) (nm)	Zeta potential (mV)
(0.01 M TA)	521	-23.97
Nanoflowers (0.05M TA)	655	-9.65
chloroplast-like (No TA)	619	-9.46
(0.01M TA) and CTAB	444	-18.58
(0.01M TA) SDS	269	-10.20

Fourier Transform Infrared Spectroscopy (FT-IR)

The presence of capping agent adsorbed on the surface of nanostructures was confirmed by FTIR spectra as shown in Figure 3A.6. The band about 472 cm^{-1} is main the characteristic stretching of Zn-O bond in all the ZnO nanostructures, which is well documented in the literature [15]. The band at 908 can be assigned to O–H out of plane bending vibration. The band at 1238 cm^{-1} can be assigned to C-O stretching in ZnO nanoparticles synthesized in presence of 0.05M tartaric acid while it was absent in ZnO nanoparticles synthesized in presence of 0.01 M tartaric acid. The band at 1399 cm^{-1} indicates NO_3^- ions adsorbed on the surface ZnO synthesized from a zinc precursor (zinc nitrate). The band about 1501 cm^{-1} can be assigned to Zn-O vibration in all the ZnO nanostructures. The broad band at 1583 cm^{-1} can be assigned to the asymmetric stretch of COO- synthesized in presence of tartaric acid. This could be due low concentration of tartaric acid adsorbed on the surface of nanoparticles. The band at 1665 and 1669 cm^{-1} can be assigned to the COO^- asymmetric stretching in ZnO nanoparticles synthesized in 0.01 M and 0.05M tartaric acid respectively. The band around 1700 cm^{-1} can be assigned to C=O, in nanostructures tartaric acid capped while it was absent in case of nanostructures synthesized without tartaric acid. The band around 2360 cm^{-1} may be due to absorbed CO_2 on the surface of nanoparticles.

The band at 2925 cm^{-1} which can be assigned to C-H stretches of the adsorbed tartaric acid. The band around 3500 cm^{-1} can be assigned to O-H stretching which indicates that nanostructures have water or hydroxyl group probably on the surface.

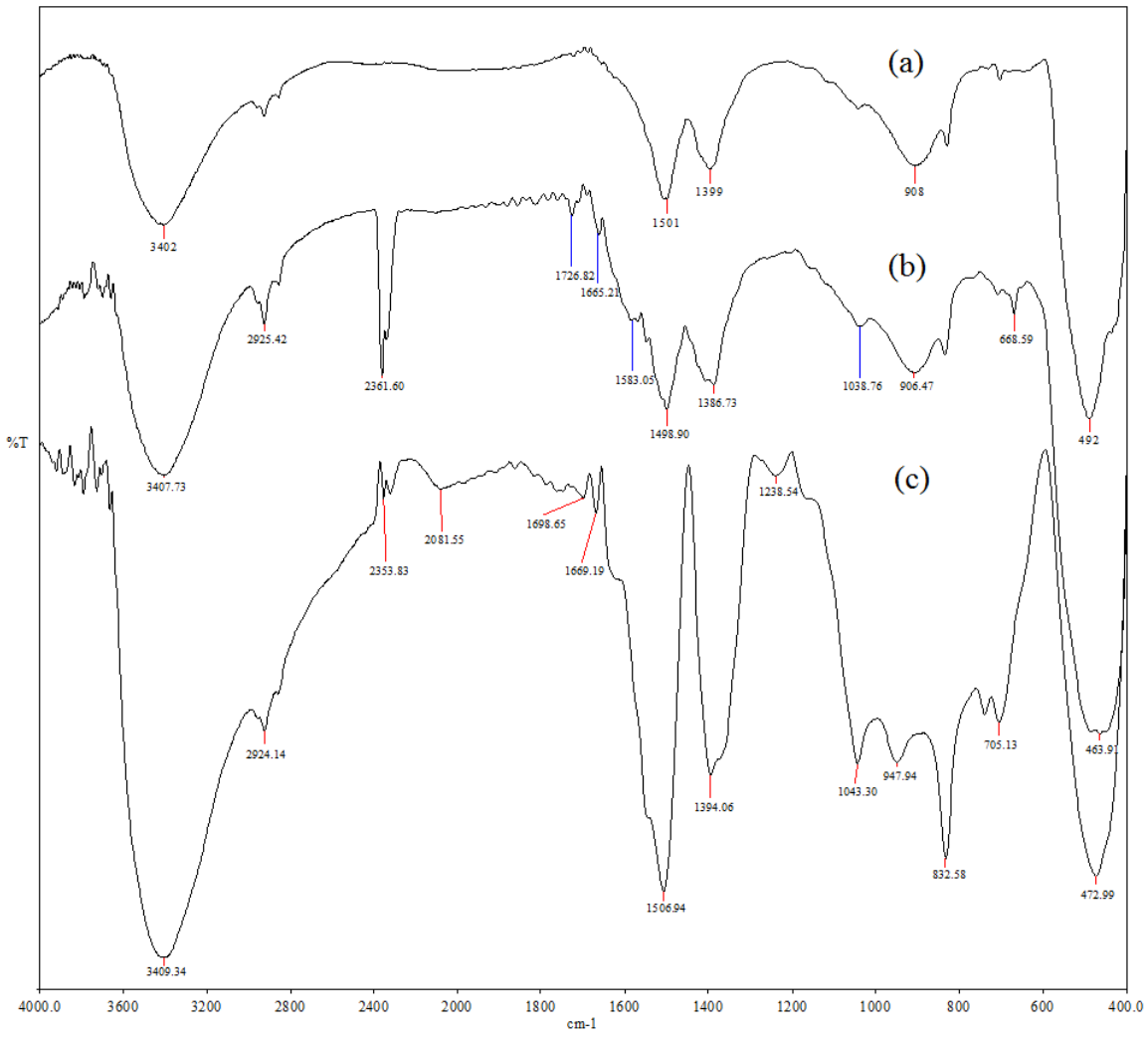

Figure 3A.6. FTIR spectra of ZnO nanoparticles with (a) chloroplast like ZnO (No TA) (b) Nanoflower (0.01M TA) (c) Nanoflowers with small petals (0.05M TA).

Optical study

The UV absorption measurement was done at room temperature as shown in Figure 3A.7 and absorption peak values are given in the Table. 3A.1. The ZnO nanoflower exhibit an excitonic absorption peak at 371 nm, which is blue-shifted when compared with the bulk ZnO (380 nm). The nanostar exhibit an excitonic absorption peak at 375 nm. The nanoprism exhibit an excitonic absorption peak at 382 nm. The chloroplast exhibit an excitonic absorption peak at ~383 nm. The chloroplast-like ZnO nanostructures exhibit an excitonic absorption peak at 375 nm. The ZnO armed-chloroplast exhibit an excitonic absorption peak at 367 nm. The ZnO nanoflower (small petals 0.05 M TA) exhibit an excitonic absorption peak at 371 nm.

Figure 3A.8 shows the photoluminescence (PL) emission spectrum of ZnO nanoparticles at room temperature. The ZnO nanoparticles of different morphologies showed emission band centered at 548 nm and 605 nm. The green emission band (548 nm) can be assigned to oxygen vacancies and this emission results from the radiative recombination of a photogenerated hole with an electron occupying the oxygen vacancy [16]. A broad yellow-orange emission band at 605 nm is observed. The origin of orange emission seems to involve point defects such as interstitial oxygen ions [17]. All the ZnO nanostructures showed emission with different intensity. Starlike ZnO nanostructures showed highest intensity of emission. The increase in tartaric acid concentration and surfactants enhanced the PL emission. The chloroplast shaped ZnO nanostructures synthesized without Tartaric acid showed intermediate emission intensity. From this we can conclude that luminescence properties can be controlled by changing the morphologies as well capping agent.

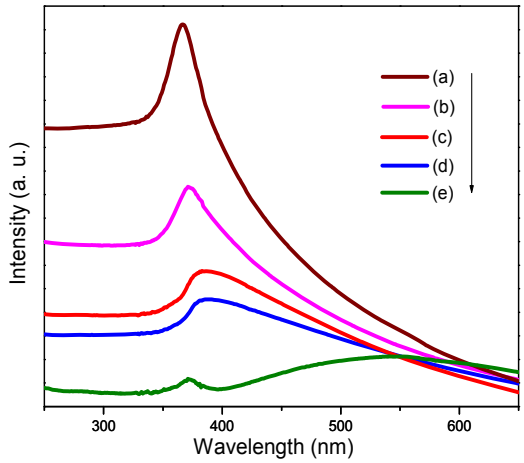

Figure 3A.7. UV-visible absorption of ZnO nanoparticles with (a) armed-chloroplast like (0.01M TA and 0.01M SDS) (b) Nanoflower (0.01M TA) (c) prism-like (0.01M TA and 0.01M CTAB) (d) chloroplast like ZnO (No TA) (e) Nanoflowers with small petals (0.05M TA).

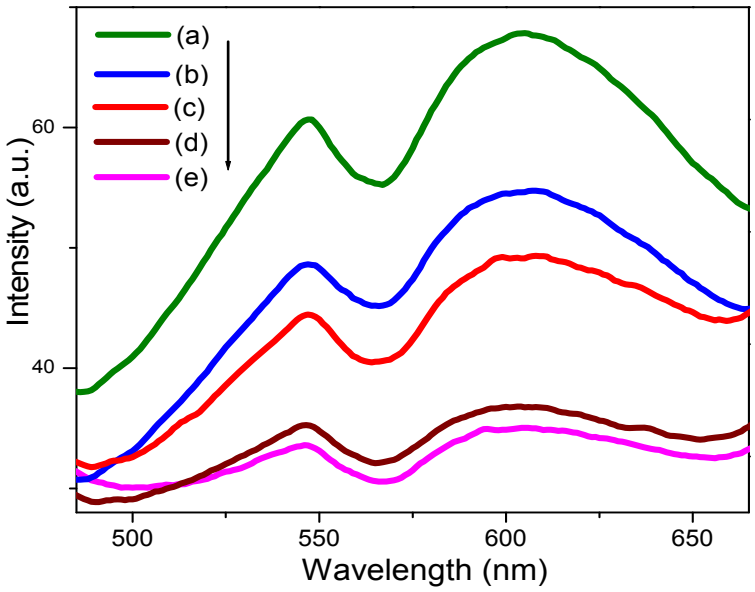

Figure 3A.8 Photoluminesence of ZnO nanoparticles synthsized in prescense (a) Nanoflowers with small petals (0.05M TA) (b) chloroplast like ZnO (No TA) (c) prism-like (0.01M TA and 0.01M CTAB) (d) armed-chloroplast like (0.01M TA and 0.01M SDS) (e) Nanoflower (0.01M TA).

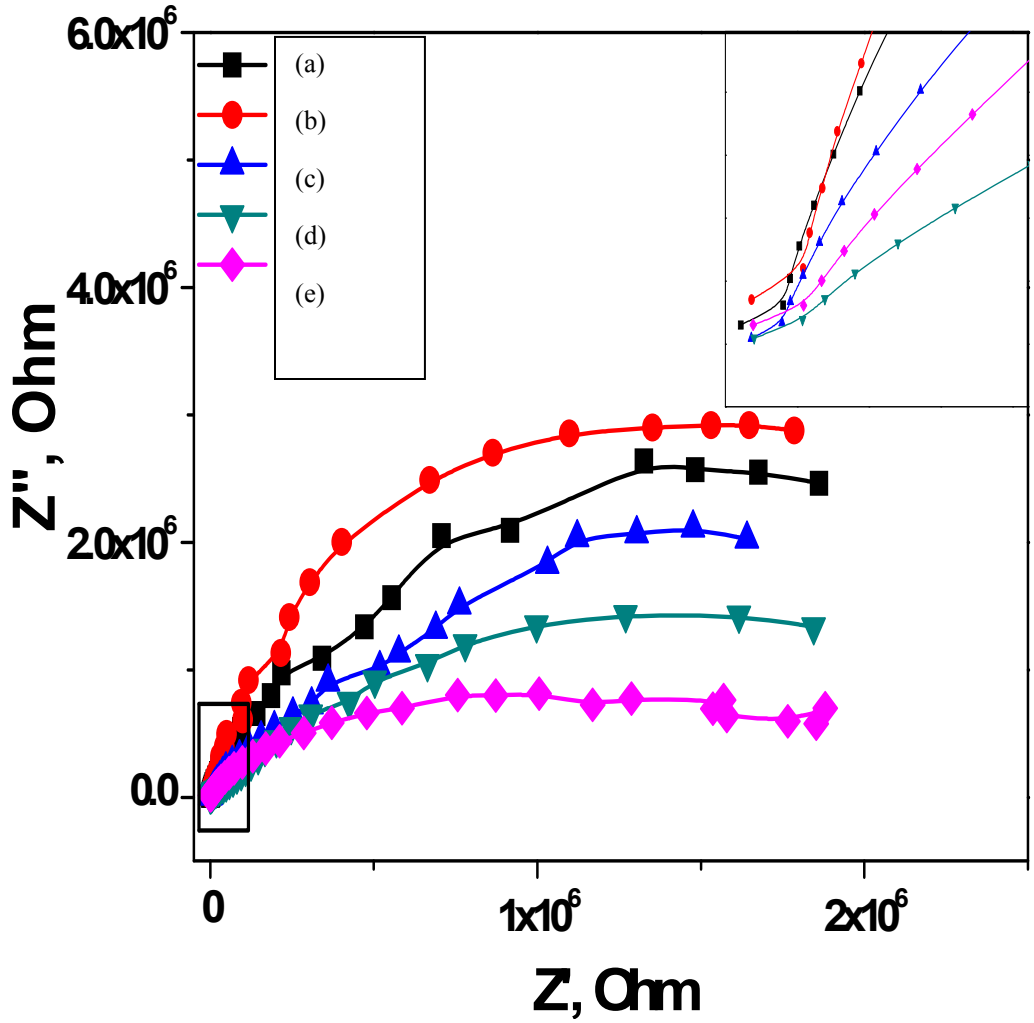

Figure 3A.9 Electrical conuctance of ZnO nanoparticles synthsized in prescense of (a) Nanoflower (0.01M TA) (b) Nanoflowers with small petals (0.05M TA) (c) chloroplast like ZnO (No TA) (d) prism-like (0.01M TA and 0.01M CTAB) (e) armed-chloroplast like (0.01M TA and 0.01M SDS).

Electrical Study

Figure 3A.9 shows the electrical conductance of ZnO nanoparticles. The ZnO nanoparticles (0.01 M TA) showed the highest electrical conductance when compared with the other ZnO nanoparticles synthesized in different concentration of TA. The ZnO nanoparticles synthesized in presence of additives (surfactant) showed lowest conductance. From the conductance study, we can conclude that the conuctance of a material depends on the morphology.

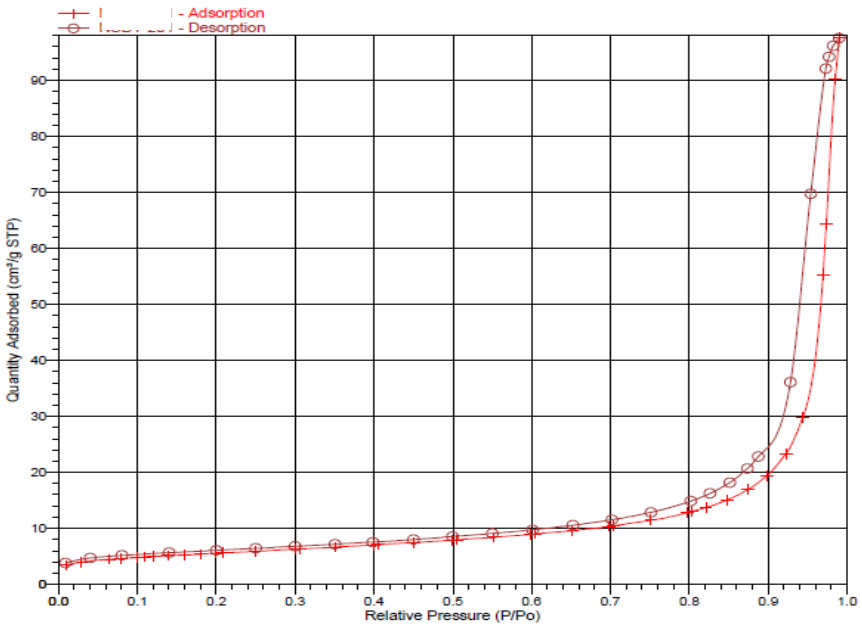

Figure 3A.10 Nitrogen adsorption-desorption isotherms for ZnO NPs with 0.01 M TA.

Table. 3A.4 BET surface characterization of ZnO nanoparticles.

Parameters	ZnO nanoflower (0.01 M TA)	ZnO nanoflower (0.05 M TA)	ZnO (0.01 M TA and SDS)
S_{BET} (m^2/g)	19.4758	21.8530	22.1758
Average pore diameter (Å)	310.0253	319.1078	157.1554
Pore volume (cm^3/g)	0.150950	0.174336	0.087126

Brunauer-Emmett-Teller (BET) specific surface area (SBET)

The nitrogen adsorption-desorption isotherms for of the ZnO NPs is shown in Figure. 3A.10, their calculated BET surface area and pore volumes are presented in Table 3A.4. ZnO NPs synthesized in 0.01 M TA and SDS showed highest surface area in comparision to the other ZnO NPs.

Conclusion

We have successfully developed a simple wet chemical method using tartaric acid as a capping agent. We obtained different morphologies such as chloroplast-like, flower-like, flower with small petal-like, prism-like and armed chloroplast-like ZnO nanostructures by changing synthetic parameters like concentration of capping agent and presence of additives like SDS and CTAB. The surface stabilization of ZnO nanostructures was studied by zeta potential. The as-synthesized nanostructures showed green and orange emission bands. The optical study shows that ZnO nanostructures may find applications in photoluminescence devices.

References

[1] B.Q. Cao, W.P. Cai, *J. Phys. Chem. C* **2008**, 112, 680.

[2] B. Li, Y. Wang, J. Phys. Chem. C 2010, 114, 890.

[3] S. Sakohara, M. Ishida, M. A. Anderson, *J. Phys. Chem. B* **1998**, 102, 10169.

[4] R. Viswanatha, S. Sapra, B. Satpati, P. V. Satyam, B. N. Dev, D. D. Sarma, *J. Mater. Chem.* **2004**, 14, 661.

[5] S. Monticone, R. Tufeu, A. V. Kanaev, *J. Phys. Chem. B* **1998**, 102, 2854.

[6] K. Vanheusden, W.L. Warren, C.H. Seager, D.R. Tallant, J.A. Voigt, B.E. Gnade, *J. Appl. Phys.* **1996**, *79*, 7983.

[7] D. Li, Y.H. Leung, A.B. Djurisic, Z.T. Liu, M.H. Xie, S.L. Shi, S.J. Xu, W.K. Chan, *Appl. Phys. Lett.* **2004**, 85, 1601.

[8] R. Jenkins, R.L. Snyder, *Introduction to X-ray powder diffractometry*, John Wiley and sons. NewYork, **1996**.

[9] B. Li, Y. Wang, *J. Phys. Chem. C* **2010,** 114, 890.

[10] Q. Yu, W. Fu, C. Yu, H. Yang, R. Wei, M. Li, S. Liu, Y. Sui, Z. Liu, M. Yuan, G. Zou, G. Wang, C. Shao, Y. Liu, *J. Phys. Chem. C* **2007,** 111, 17521.

[11] S. Cho, J-W Jang, J. S. Lee, K-H. Lee, *Langmuir* **2010**, 26, 14255.

[12] H. Zhang, D. Yang, D. Li, X. Ma, S. Li, D. Que, *Cryst. Growth Des.* **2005**, 5, 547.

[13] U. Pal, P. Santiago, *J. Phys. Chem. B* **2005**, 109, 15317.

[14] J.M. Berg, A. Romoser, N. Banerjee, R. Zebda, C.M. Sayes, *Nanotoxicology* **2009**, 3, 276.

[15]. S. Maensiri, P. Laokul, V. Promarak, *J. Cry. Growth* **2006**, 289, 102.

[16] H. M. Cheng, H. C. Hsu, Y. K. Tseng, L. J. Lin, W. F. Hsieh, *J. Phys. Chem. B* **2005**, 109, 8749.

[17] M. Liu, A. H. Kitai, P. Mascher, *J. Lumin.* **1992**, 54, 35.

3B. 1 Introduction

The optical properties of ZnS nanoparticles can be tuned by controlling the particle size, shape, surface properties and presence of dopant ions. The introduction of metal ions such as Mn, Cu, Ni, Li, Eu into the host matrix results into doped nanoparticles. These doped semiconductor nanoparticles find application as dilute magnetic semiconductors (DMS). Bhargava et al. suggested that the hybridization of the s-p electron orbital of the ZnS host and the d electron orbital of the Mn^{2+} ion accounts for the lifetime shortening and increase in the luminescence [1]. ZnS:Mn^{2+} [2] show orange emission and ZnS:Cu^{2+} show blue-green emission property[3].

In present study, we have synthesized doped and undoped ZnS nanoparticles using ±(DL)-Tartaric acid as capping ligand by wet-chemical method. The effect of liquor ammonia (as an additive) on the particle size is also studied. Optical properties of the as-synthesized nanoparticles have been studied and correlated with dopants.

3B. 2 Experimental

Synthesis

In a round bottom flask 25 ml aqueous solution of $Zn(NO_3)_2$ (0.2 M) and 25 ml aqueous solution of $Ni(CH_3COO)_2.4H_2O$ (4.4×10^{-4} M) were mixed. To this solution 50 ml aqueous solution of of tartaric acid (0.01M) was added. The reaction mixture was stirred for half an hour to make it homogeneous. Then 50 ml of 0.1 M sodium sulphide solution was added dropwise and the mixture was further stirred for 3 h to get a homogenous stabilized dispersion. The resulting dispersion was centrifuged at 8000 rpm, washed with deionised water (three times) and then dried at 60 °C to obtain a powder. Similarly in case of Mn^{2+} doped and Co^{2+} doped ZnS nanoparticles 25 ml aqueous solution of $Mn(CH_3COO)_2.4H_2O$ (4.7×10^{-4} M) and $CoCl_2.6H_2O$ (4.7×10^{-4} M) were used respectively. The undoped ZnS nanoparticles were synthesized keeping the other conditions same as above. For ZnS nanoparticles synthesized in

presence of NH_3 as an additive, 14 ml of liquor ammonia (13.4 M) was added with tartaric acid maintain the other parameters same as in case of undoped ZnS nanoparticles.

3B.3 Results and discussions

X-ray diffraction (XRD)

The crystallanity and purity of the as-synthesized undoped and M^{+2} (M= Mn, Ni and Co) doped ZnS nanoparticles have been studied by X-ray diffraction (XRD) pattern shown in Figure 3B.1. The diffraction pattern matches with the standard ZnS zinc blende phase (JCPDS card no. 65-0309). The broadening of XRD peaks indicates particle size in the nano-regime. The major diffraction peaks correspond to (111), (220), and (311) of ZnS crystals facets, respectively. The average particle sizes were calculated using Debye-Scherrer formula [4]. The absence of any other phase in the XRD pattern indicates high purity of the nanoparticles. The calculated particle size was in the range of 2.0-6.0 nm as shown in Table 1. The undoped ZnS nanoparticles synthesized in presence of ammonia showed lowest particle size when compared with the other samples. This suggests that ammonia also controls the particle size along with the tartaric acid.

Energy Dispersive X-ray (EDX)

Elementary composition of the doped and undoped ZnS nanoparticles were studied by Energy Dispersive X-ray (EDX) analysis (Figure 3B.2). From EDX analysis, it can be observed that the compositions of the nanoparticles depends on dopant concentration (Table 3B.2). The stoichiometric ratio for undoped and ZnS:Mn^{2+} is almost 1. The EDX analysis of ZnS:Co^{2+} nanoparticles indicates sulphur defficiency and relatively low % of doping compared with ZnS:Mn^{2+} nanoparticles.

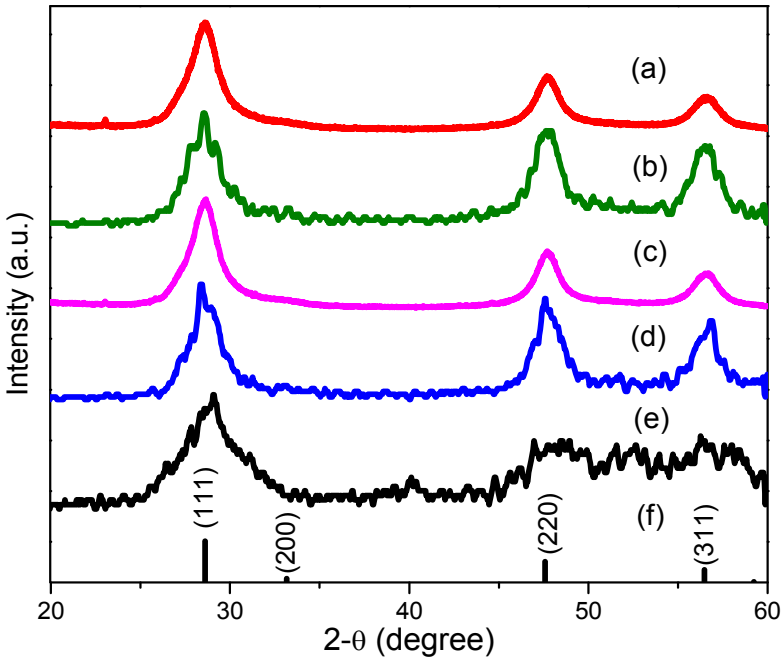

Figure. 3B.1 The XRD pattern of nanoparticles (a) ZnS:Co^{2+} (b) ZnS:Ni^{2+} (c) ZnS:Mn^{2+} (d) undoped ZnS (e) undoped ZnS (NH_3 as additive) nanoparticles (f) Bulk ZnS zinc blende phase (JCPDS card no. 65-0309).

Table 3B.1. Absorption edge, band gap energy and particle size of ZnS nanoparticles calculated using Debeye-Scherrer formula.

Sample	Absorption edge (nm)	Band gap energy E_g (eV)	Particle size (nm)
undoped ZnS	324	3.83	4.4
ZnS:Ni^{2+}	323	3.85	4.0
ZnS:Mn^{2+}	325	3.82	5.8
ZnS:Co^{2+}	325	3.82	4.0
undoped ZnS (NH_3 as additive)	320	3.88	2.4

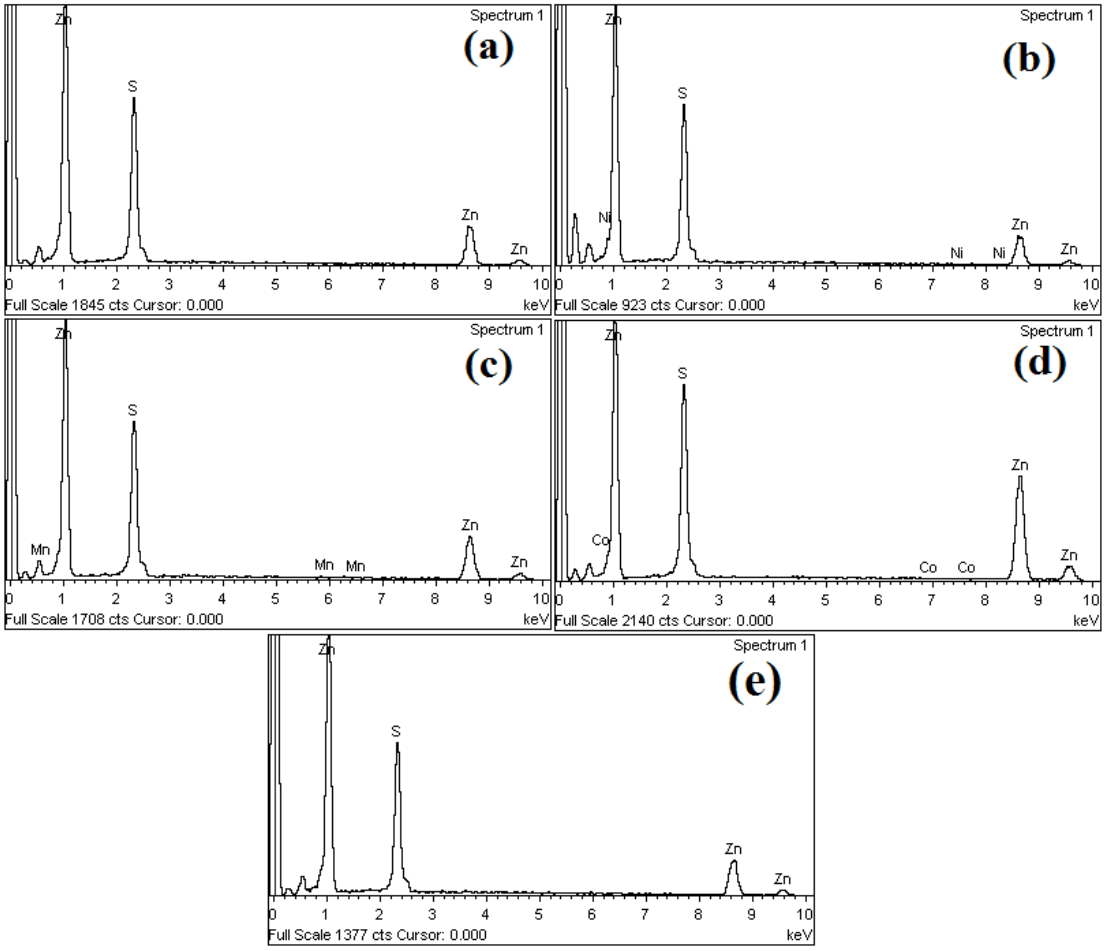

Figure. 3B.2 The EDX analysis spectra of (a) undoped ZnS (b) ZnS:Ni^{2+} (c) ZnS:Mn^{2+} (d) ZnS:Co^{2+} (e) undoped ZnS (NH_3 as additive) nanoparticles.

Table 3B.2. Elementary composition of the undoped and doped ZnS nanoparticles as studied by EDX.

Sample	Zinc (at. %)	Sulphur (at. %)	Dopant (at. %)
undoped ZnS	48.63	51.37	-
ZnS:Mn^{2+}	48.81	50.89	0.29
ZnS:Co^{2+}	61.32	38.63	0.06
ZnS:Ni^{2+}	49.06	50.69	0.25
undoped ZnS (NH_3 as additive)	51.39	48.61	-

Transmission Electron Microscopy (TEM)

The particle size and morphology of the as-synthesized nanoparticles was studied by TEM as shown in Figure 3B.3. From the TEM image of undoped ZnS nanoparticles, it can be observed that a cluster of about 64.6 nm is formed by fusing small spherical nanoparticles of size in the range of 9.3 nm. The SAED pattern shows a crystalline nature of the material (Figure 3 inset) which is supported by the XRD results.

Optical study

UV absorption spectra of as-synthesized nanoparticles are shown in Figure 3B.4. The absorption edge of the M^{+2} (M= Mn, Ni and Co) doped and undoped ZnS nanoparticles showed blue shift when compared with the bulk ZnS material. The blue shift of absorption edge is due to quantum confinement effect [5]. The absorption edge of undoped ZnS nanoparticles synthesized in presence of tartaric acid and ammonia showed the highest blue shift when compared with the undoped and doped ZnS nanoparticles. The band gap energy of the as synthesized materials was in the range of 3.82-3.88 eV (Table 1).

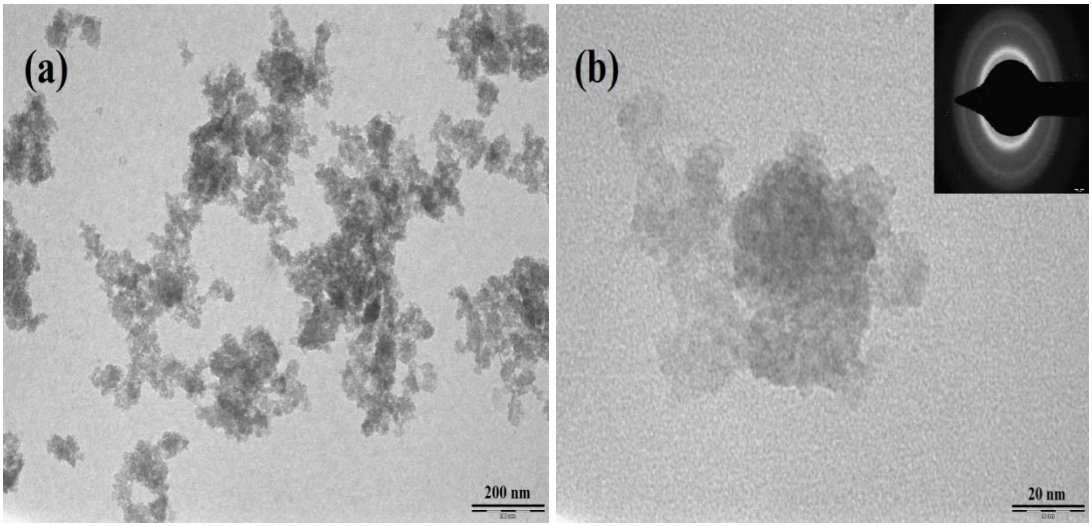

Figure. 3B.3 TEM image of the undoped ZnS nanoparticles prepared in the precence of Tartaric acid at different magnification and inset shows the selected area electron diffraction pattern.

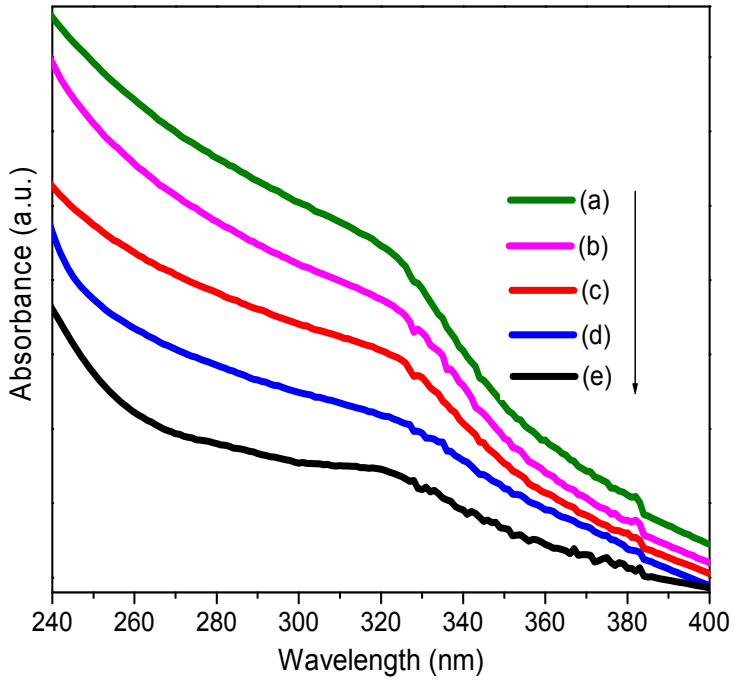

Figure. 3B.4 Absorption spectra of (a) ZnS:Ni^{2+} (b) ZnS:Mn^{2+} (c) ZnS:Co^{2+} (d) undoped ZnS (e) undoped ZnS (NH_3 as additive) nanoparticles.

The PL emission spectra of doped and undoped ZnS nanoparticles are shown in Figure 3B.5. sharp emission band of different intensity at 330 nm can be observed from doped and undoped ZnS nanoparticles. ZnS:Co^{2+} shows highest peak intensity at 330 nm, undoped ZnS nanoparticles showed intermediate intensity, ZnS:Mn^{2+} and ZnS:Ni^{2+} nanoparticles showed lowest PL intensity. This band can be attributed to band to band transition [6]. A emission band at 350 nm was observed in case of undoped ZnS and ZnS:Co^{2+} nanoparticles. A red shift of 5-10 nm was observed in case of ZnS:Ni^{2+} and ZnS:Mn^{2+} nanoparticles. This band can be assigned to near band-edge transitions [7]. The ZnS:Mn^{2+} nanoparticles showed highest intensity of this band. In case of ZnS:Mn^{2+} nanoparticles a weak emission band at 400 nm was observed, which is due to recombination of electrons from the energy levels of sulfur vacancies (neutral donor) with the holes from the valence band [8].

The ZnS:Mn^{2+} nanoparticles showed highest intensity peak at 470 nm succeed from ZnS:Ni^{2+} and undoped ZnS nanoparticles showed emission band of intermediate intensity. In case of ZnS:Co^{2+} nanoparticles quenching was observed. A broad band at 485 nm was observed in doped and undoped ZnS nanoparticles, corresponds to transfer of electron vacancy (sulphur) to Zn defect states [9]. A broad band at 495 nm was observed in doped and undoped ZnS nanoparticles, which is assigned to zinc ions at the surface of the nanoparticles [10]. The PL emission study shows that the optical property of host material can be tuned by doping different transition metal ions. This tuning of the optical property may find application in the future optical devices and sensors.

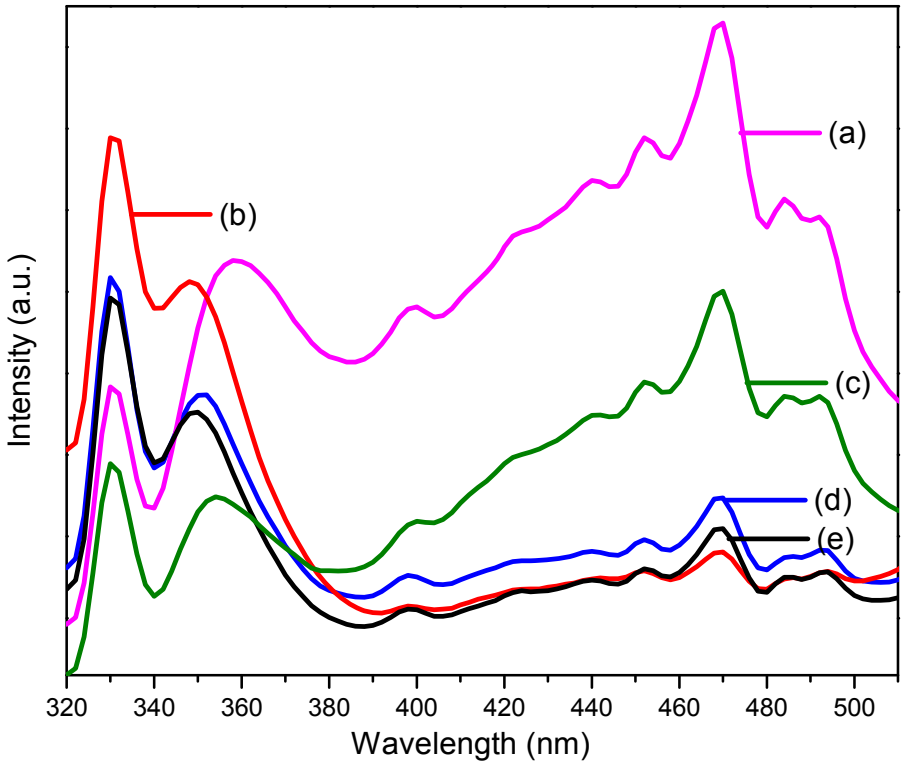

Figure. 3B.5 Photoluminescence emission spectra of (a) ZnS:Mn^{2+} (b) ZnS:Co^{2+} (c) ZnS:Ni^{2+} and (d) undoped ZnS (e) undoped ZnS (using NH_3 as an additive).

Fourier Transform Infrared Spectroscopy (FT-IR)

The presence of tartaric acid on the surface was confirmed by FTIR spectroscopy as shown in Figure 3B.6. A small band at 484 cm^{-1} can be assigned to metal–oxygen. The band at 619 cm^{-1} can be assigned to C–S linkages which occur in the region of 700–600 cm^{-1}. The band at 712 cm^{-1} can be assigned to methylene rocking vibration. The band at 1116 is due to C-H stretching. The band at 1384 cm^{-1} is due to C-O stretching. The band at 1619 cm^{-1} is due to asymmetrical COO^- stretching. The absence of peak about 1700 cm^{-1} indicates that free tartaric acid is absent. The broad band at 3407 cm^{-1} is due to O-H stretching.

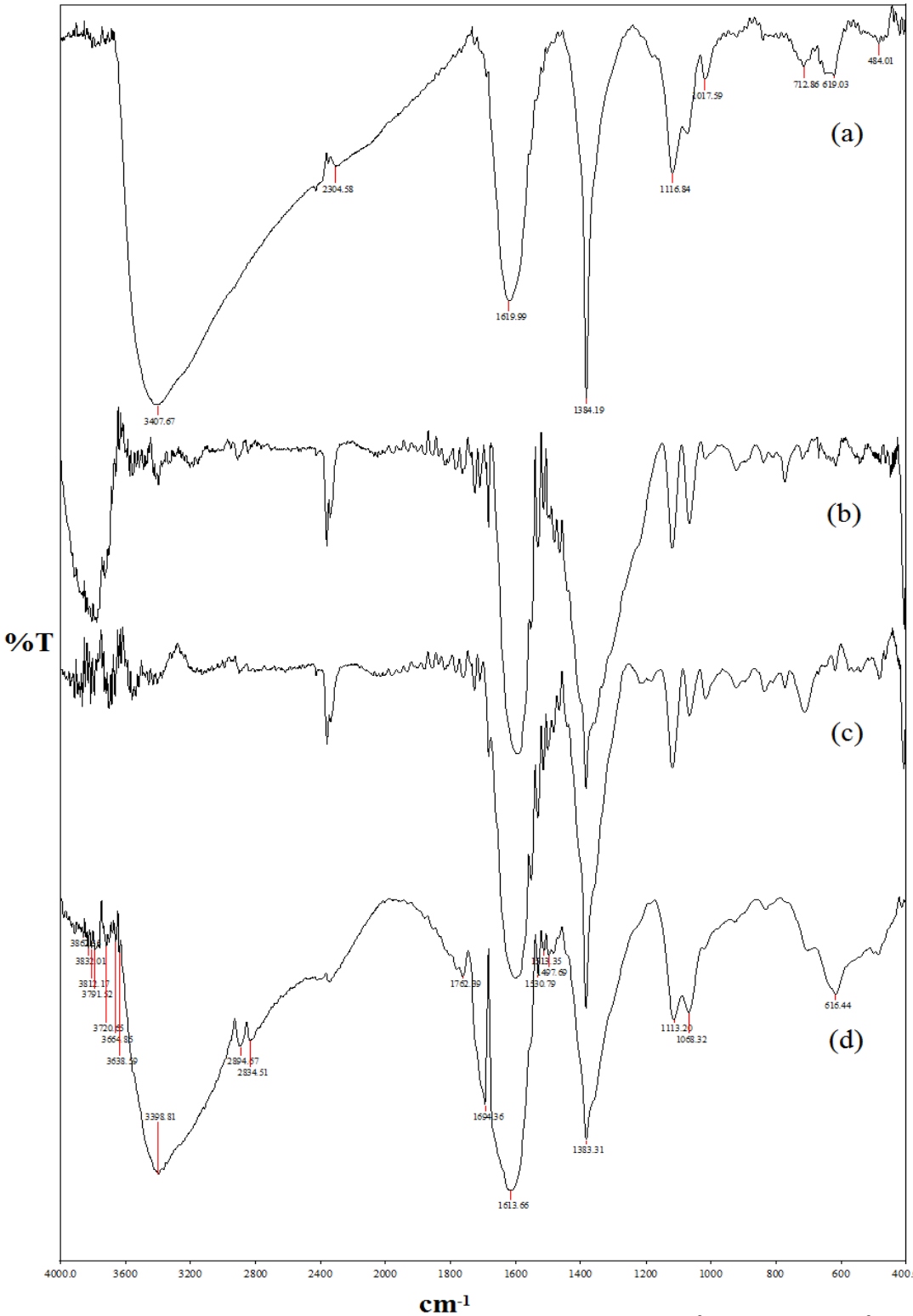

Figure. 3B.6 FTIR spectra of (a) undoped ZnS (b) ZnS:Ni^{2+} (c) ZnS:Mn^{2+} (d) ZnS:Co^{2+} nanoparticles synthesized in presence of tartaric acid.

Conclusion

We have successfully synthesized Mn^{+2}, Ni^{+2}, Co^{+2} doped and undoped ZnS nanoparticles by wet chemical method. Tartaric acid was used as capping agent. The TEM analysis showed nearly spherical shaped nanoparticles. The ZnS:Mn^{2+} nanoparticles showed highest photoluminescence emission intensity when compared with the undoped ZnS nanoparticles. The optical study shows that these materials can be used in future nano-devices.

References

[1] R.N. Bhargava, D. Gallagher, X. Hong, A. Nurmikko, *Phys. Rev. Lett.* **1994**, 72, 416.

[2] B.B. Srivastava, S. Jana, N.S. Karan, S. Paria, N.R. Jana, D.D. Sarma, N. Pradhan, *J. Phys. Chem. Lett.* **2010**, 1, 1454.

[3] A. Klausch, H. Althues, C. Schrage, P. Simon, A. Szatkowski, M. Bredol, D. Adam, S. Kaskel, *J. Lumin.* **2010**, 130, 692.

[4] R. Jenkins, R.L. Snyder, *Introduction to X-ray powder diffractometry* (John Wiley and sons, NewYork, **1996**).

[5] R. Rossetti, R. Hull, J.M. Gibson, L.E. Brus, *J. Chem. Phys.* **1985**, 82, 552.

[6] J.X. Ding, J.A. Zapien, W.W. Chen, Y. Lifshitz, S.T. Lee, *Appl. Phys. Lett.* **2004**, 85, 2361.

[7] N. Chestnoy, R. Hull, L.E. Brus, *J. Chem. Phys.* **1986**, 85, 2237.

[8] W.G. Becker, A.J. Bard, *J. Phys. Chem.* **1983**, 87, 4888.

[9] K. Manzoor, S.R. Vadera, N. Kumar, T.R.N. Kutty, *Solid State Commun.* **2004**, 129, 469.

[10] D.E. Dunstan, A. Hagfeldt, M. Almgren, H.O.G. Siegbahn, E. Mukhtar, *J. Phys. Chem.* **1990**, 94, 6797.